



Magnetic resonance detects brainstem changes in chronic, active heavy drinkers

Courtney W. Bloomer^a, Daniel D. Langleben^b, Dieter J. Meyerhoff^{c,*}

^aUniversity of Pennsylvania-Presbyterian Medical Center, Philadelphia, PA 19104, USA

^bTreatment Research Center, Department of Psychiatry, University of Pennsylvania Health Services, Philadelphia, PA 19104, USA

^cDepartment of Radiology University of California, San Francisco and Magnetic Resonance Unit,

Department of Veterans Affairs Medical Center, 4150 Clement Street, 114M, San Francisco, CA 94121, USA

Received 30 October 2003; received in revised form 3 June 2004; accepted 5 June 2004

Abstract

Neuropathological and neuroimaging studies show cortical and subcortical volume loss in alcohol-dependent individuals. Using quantitative magnetic resonance imaging (MRI) and proton magnetic resonance spectroscopic imaging (¹H MRSI), we studied the size and potential cellular injury of the brainstem in untreated heavy alcohol drinkers. The brainstem is considered critical in the development and maintenance of drug and alcohol dependence. Two methods of brainstem size determination were compared: standard volumetry vs. midsagittal MR image area measurement. Heavy drinkers ($n=12$) and light drinkers ($n=10$) were compared with MRI; ¹H MRSI brainstem data were obtained from a subset of this cohort. Chronic heavy drinking was associated with significantly smaller midsagittal areas of the brainstem, midbrain, and pons, and with significantly smaller overall brainstem volume. Heavy drinking was also associated with significantly lower ratios of *N*-acetyl-aspartate and choline-containing metabolites compared with creatine-containing compounds in the brainstem, independent of brainstem atrophy. Additionally, brainstem volume and midsagittal brainstem area were correlated ($r=0.78$). These structural and metabolite findings are consistent with neuronal injury in the brainstem of untreated chronic heavy drinkers. The results also indicate that the midsagittal MRI brainstem area is an easily determined and reliable indicator of brainstem volume.

© 2004 Elsevier Ireland Ltd. All rights reserved.

Keywords: MRI; MRS; Alcohol; Brainstem; HIV; Serotonin

1. Introduction

Chronic heavy alcohol consumption is associated with smaller regional brain volumes, functional and metabolic deficits. A reduction in brain volume has been demonstrated in neuroimaging and pathological

* Corresponding author. Tel.: +1 415 221 4810x4803; fax: +1 415 668 2864.

E-mail address: djmey@itsa.ucsf.edu (D.J. Meyerhoff).

studies, most often in cortical gray matter, frontal and parietal white matter, cerebellum, mesial temporal lobe, subcortical structures, corpus callosum, and mammillary bodies (Picciotto and Corrigan, 2002; Scroop et al., 2002; Sullivan, 2000; Kilts et al., 2001; Pfefferbaum et al., 1995). The brainstem is comprised of midbrain (mesencephalon), pons and medulla (Duvernoy, 1995), which contain white matter tracts and gray matter nuclei that play crucial roles in autonomic and motor function, as well as in conditioning, learning and, ultimately, addiction (Erhardt et al., 2002; Pfefferbaum et al., 2002b; Sziraki et al., 2002). Recent neuroimaging studies indicate volume loss in the brainstem, in particular in the pons of abstinent alcoholics (Sullivan et al., 2003; Pfefferbaum et al., 2002b; Sullivan and Pfefferbaum, 2001; Kuruoglu et al., 1996). Additional brainstem injury has not been fully characterized.

In vivo proton magnetic resonance spectroscopic imaging (^1H MRSI) is routinely used to measure signals from naturally occurring metabolites in the brain, including *N*-acetyl-aspartate (NAA), choline-containing metabolites (Cho), and creatine-containing metabolites (Cr). NAA is an amino acid that occurs in mature neurons only [although it has been detected in oligodendrocytes in vitro (Bhakoo and Pearce, 2000)]. Lower NAA or NAA/Cr ratio is generally interpreted to reflect loss of or injury to neurons and has been reported in numerous neuropsychiatric disorders, including alcohol abuse. Cho changes reflect alterations in cellular membrane integrity, and elevated Cho or Cho/Cr is used as an indicator of increased cell turnover, myelin breakdown, gliosis, or inflammation. Cr is useful for evaluating cellular metabolism and energy storage, and is generally well-regulated and relatively stable in most disease processes (Macmillan et al., 2002; Garnett et al., 2001). Whereas most ^1H MRSI studies of the brainstem have focused on healthy controls (Hanstock et al., 2002; Mascalchi et al., 2002), a recent study of active chronic heavy drinkers found a negative association between brainstem NAA and lifetime alcohol consumption (Meyerhoff et al., 2004).

The goals of this study were to determine the size of the brainstem and its substructures in heavy alcohol drinkers using volumetric magnetic resonance imaging (MRI) and to investigate possible glial and neuronal changes in the brainstem of these individuals

using ^1H MRSI. Our primary hypothesis was that chronic alcohol use would be associated with a smaller brainstem and cellular brainstem injury. A third goal was to evaluate and compare two methods of brainstem size assessment. MR images can be used to approximate the volume of various brain structures by adding the areas of interest on contiguous MRI slices and multiplying by slice thickness. A less labor-intensive approach postulates that the area of a single midsagittal slice in a symmetrical brain structure is a reliable estimate of its volume. For example, in developmentally delayed patients, it has been shown that the midsagittal slice areas of the pons and medulla on MRI can be measured reliably and are significantly correlated with their respective volumes (Aylward and Reiss, 1991). Thus, we hypothesized that the midsagittal slice area of the entire brainstem is well correlated with total brainstem volume and, therefore, reliably represents brainstem volume in this study group.

2. Methods

2.1. Participants

The study was approved by the Institutional Review Boards of the University of California, San Francisco and the Veterans Affairs Medical Center. Twenty-two alcohol-using men were recruited from the community using advertisement and gave informed consent before study participation. None were in treatment for substance abuse (including alcohol use disorder) or seeking treatment at the time of the study. Individuals with a history of medical, neurological, psychiatric disorders, or contraindications to MRI were excluded; HIV infection was not an exclusion criterion. Lifetime drinking history was assessed with standard measures (Sobell et al., 1988; Skinner and Sheu, 1982; Skinner, 1979). Light drinking was defined as drinking an average of fewer than 30 standard alcoholic drinks (equivalent of 13.6 g of 100% ethanol) a month over the lifetime while heavy drinkers consumed at least 80 alcoholic drinks per month for more than 2 years prior to the study. The participants were divided into light drinkers (LD, $n=10$, age 44.5 ± 7.4 years) and age-matched heavy drinkers (HD, $n=12$, age 46.8 ± 5.1 years, $P < 0.4$). LD

averaged 17 ± 9 drinks/month (range 5–30) and HD consumed 234 ± 182 drinks/month (range 80–600, median 157), more than 14 times as much as LD ($P=0.002$). Of the 22 participants, six were HIV-seropositive without AIDS-defining diagnosis except for one LD. All participants underwent structural MRI, whereas ^1H MRSI was obtained in a subset of nine LD (4 HIV-positive) and six age-matched HD (2 HIV-positive). Alcohol consumption was similar between HIV-negative and HIV-positive samples within each group.

2.2. Data acquisition

2.2.1. MRI

MR data were obtained on a Siemens Vision 1.5 T scanner. Two different sets of images were obtained: oblique axial images along a plane connecting the anterior and posterior commissures as seen on midsagittal scout images and oblique coronal images, perpendicular to the long axis of the hippocampus as seen on lateral sagittal scout images. The axial scan was acquired as a contiguous interleaved double spin-echo (DSE) (TR/TE=2575/20/80 ms) with a 3-mm slice thickness and no slice gap. Sixteen participants had a DSE acquired with an in-plane spatial resolution of $1 \times 1 \text{ mm}^2$; the DSE for the remaining six participants had an in-plane image resolution of $0.938 \times 0.938 \text{ mm}^2$. The oblique coronal images were obtained using a 3D gradient echo MRI sequence (MP-RAGE, TR/TE/TI=10/4/250 ms) with a slice thickness of 1.5 mm. The in-plane resolution was $1.409 \times 1.409 \text{ mm}^2$ for 16 participants, and $1.5 \times 1.5 \text{ mm}^2$ for the remaining six participants.

2.2.2. MRSI

A laterally restricted single slice was used to evaluate metabolites in the brainstem, hippocampi and mesial temporal lobe white matter. MR images from a short 17-slice turbo spin-echo (TSE) sequence were used (TR/TE=500/14 ms) for placement of the slice, which was angulated parallel to the long axis of the hippocampi as seen on the sagittal scout images (Fig. 1). A 15-mm-thick PRESS selected volume of interest with in-plane dimensions of $100 \times 70 \text{ mm}^2$ was then angulated parallel to the TSE slices and positioned on the TSE images to include a section of the brainstem and bilateral hippocampi. Shinnar Le

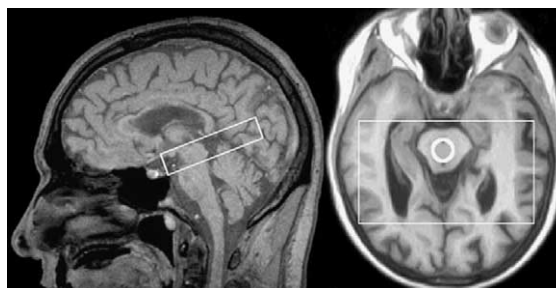


Fig. 1. Position of PRESS ^1H MRSI volume superimposed on localizer MR images. The PRESS volume on the sagittal MR image (left) was angulated along the long axis of the hippocampi as seen on parasagittal scout images. The 15-mm-thick PRESS volume with typical in-plane dimensions of $100 \times 70 \text{ mm}^2$ was positioned on coplanar TSE images to include brainstem and bilateral hippocampi (right). For brainstem ^1H MRSI data analysis, a single voxel was selected from the center of the brainstem at the level of the midbrain as indicated by a circle on the axial TSE image.

Roux excitation pulses were used for selection of optimized slice profiles and optimized water suppression. After localized shimming on this volume, a ^1H MRSI data set was acquired (TR/TE=1800/135 ms), with a field of view of $210 \times 210 \text{ mm}^2$ and a circular k -space sampling scheme with 24×24 phase encoding steps, resulting in a nominal voxel volume of 1.1 ml and a total acquisition time of 13 min. The spectral sweep width was 1000 Hz; the spectral acquisition size was 512 points (see Soher et al., 2000, for a detailed description of this protocol). All MR data were acquired in a single session lasting approximately 1.5 h.

2.3. Data processing

2.3.1. MRI

The coronal 3D T1-weighted MP-RAGE data sets were reoriented into the sagittal plane for area and volume measurements using in-house software programs. First, we selected midline intracranial landmarks (septum pellucidum, aqueduct, obex, 4th ventricle, midbrain tectum, mammillary body) on the sagittal images and placed them on the coronal and axial projections. Each individual data set was then realigned using these landmarks to produce optimal visualization of the brainstem in the mid-sagittal plane. The axial DSE scans were used to segment the brain automatically into CSF, white and gray matter using in-house software (Cardenas et al.,

2001). The sum of supratentorial gray and white matter constituted total brain tissue volume, which was used to normalize the brainstem data. The cerebellum was not included in this measure because not all participants' cerebellums were completely included in the MRI field-of-view due to Specific Absorption Rate (SAR) limitations. All MRI studies were interpreted as clinically normal by a neuro-radiologist with the exception of mild ventricular enlargement in one HIV-positive heavy drinker. Brainstem volume and midsagittal slice areas of the brainstem and its substructures (midbrain, pons and medulla) were measured with two independent slice-selection and manual-tracing techniques on resliced T1-weighted MR images: one for midsagittal slice brainstem area and one for brainstem volume measurement.

2.3.2. Brainstem area measurement

The protocol was based on previously reported methods using the midsagittal slice as a proxy for volume in midline structures, such as the cerebellum (Courchesne et al., 1994; Raz et al., 1992; Aylward

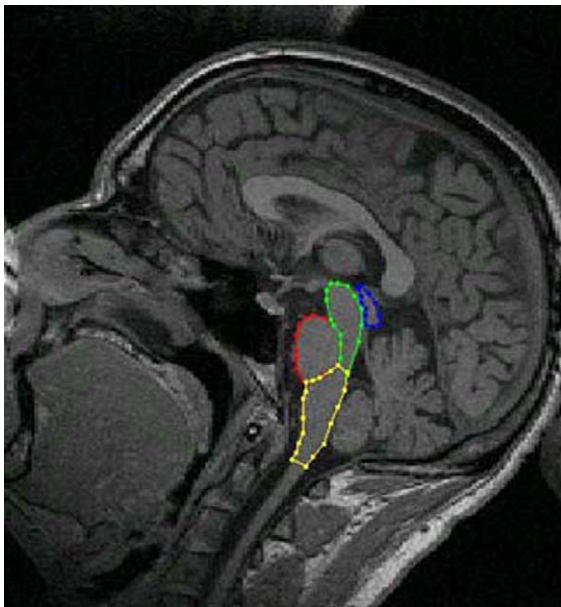


Fig. 2. Manual outline of brainstem substructures on a T1-weighted image resliced in the midsagittal plane. The midbrain is outlined in green (and includes tectum and tegmentum outlined in blue); the boundary of the pons is in red and the medulla is in yellow (for more details, see text).

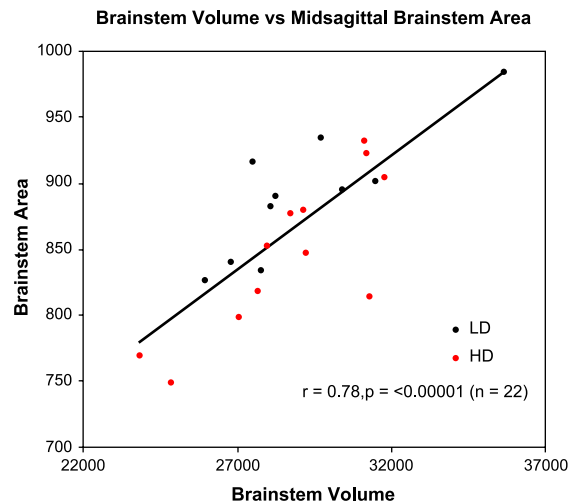


Fig. 3. The absolute measures are in arbitrary units (a.u.) derived from pixel counts. The absolute midsagittal brainstem slice area was correlated with total brainstem volume ($r=0.78$, $P<0.00001$) and was similar for LD and HD separately (both $r>0.8$, both $P<0.003$).

and Reiss, 1991) and the midbrain (Nopoulos et al., 2001). After reconstruction of T1-weighted images as described above, the midbrain tectum, the aqueduct and the fourth ventricle were used as landmarks to identify the midsagittal brainstem image. The midbrain (including tectum and tegmentum), the pons and the medulla were outlined manually (Fig. 2) using in-house software. To outline the brainstem and its substructures, a combination of anatomical and MR signal intensity criteria were used as follows: The pons was differentiated from the medulla and midbrain by signal intensity. The medulla and the midbrain were outlined by using the posterior recess of the fourth ventricle to the point of maximal curvature of the olivary body. Two independent operators, who were blinded to the participants' group membership, traced the entire data set twice. Correlations and intraclass correlation coefficients (ICC) were computed to assess the reliability of the tracing method.

2.3.3. Brainstem volume measurement

After reorientation, the entire brainstem was traced manually on the coronal slices. The superior boundary of the brainstem was a line connecting the anterior and posterior commissures. The inferior boundary was the decussation of the pyramids. The lateral boundaries were points of separation of the superior and middle

cerebellar peduncles. For the brainstem volume measurement, we did not outline substructures separately due to difficulty discerning the structures reliably on all images.

Areas and volume were calculated from pixel counts of the outlined structures, pixel size, and slice thickness. To control for the effects of overall brain size on brainstem size, all individual measurements were normalized to the individual's total supratentorial brain tissue volume (i.e. intracranial vault minus cerebellum, brainstem, and cerebrospinal fluid). As supratentorial brain tissue volume correlated significantly with brainstem volume ($r=0.77$, $P<0.0001$), this normalization assured that the brainstem measures reflected size changes that were over and above those of generalized cerebral atrophy.

2.3.4. MRSI

Data sets were zero-filled to a rectangular matrix of $32 \times 32 \times 1024$ points, Fourier-transformed, and then phase- and baseline-corrected using in-house software (Soher et al., 1998). Gaussian broadening with 4-Hz line width was used in the spectral direction and mild Gaussian apodization was applied along both spatial directions, yielding ^1H MRSI voxels of approximately 1.6-ml effective volume. In-house software was used to spatially coregister the ^1H MRSI data with the TSE images. Individual spectra were extracted in the regions of the hippocampus, temporal lobe white matter, and brainstem. In particular, a single voxel was selected from the center of the brainstem at the level of the midbrain as seen on the TSE, so as to only contain tissue from midbrain and pons in an unspecified proportion (Fig. 1). Resonances from *N*-acetyl-containing metabolites (primarily NAA) at 2.02 ppm, creatine and phosphocreatine (Cr) at 3.05 ppm, and choline-containing compounds

(Cho) at 3.25 ppm were fit to Gaussian lines using NMR1™ software (New Methods Research, Syracuse, NY) and peak integrals recorded. These integrals were corrected for variation in head coil loading and receiver gain for direct comparison among participants. Since no corrections for potential relaxation time differences between individuals or groups were applied (measuring relaxation times is prohibitively time consuming), these corrected peak areas reflect institutional concentrations. Metabolite concentrations were expressed as absolute measures and as ratios to Cr. Cr is used as an internal calibration reference in the computation of metabolite ratios to remove noise from potential instrument instabilities.

2.4. Statistical analysis

Main outcome measures for the MRI data were the normalized total brainstem volume and midsagittal slice areas of the brainstem, midbrain, pons, and medulla. In our main analyses, we evaluated heavy drinking effects via two-tailed *t*-tests between HD and LD. Effect sizes were calculated by dividing the difference of group means by the mean of their standard deviations. In secondary analyses, we evaluated the main effects of heavy drinking and HIV infection using a two-factor (alcohol and HIV status) analysis of variance (ANOVA, SAS General Linear Models Procedure). Spearman ranked tests assessed correlations between the normalized MRI measures and drinking status, and among different absolute MRI measures. To determine interrater reliability of our brainstem measures, we used Pearson correlations between the manual structure tracings of brainstem measurements from two raters and calculated the corresponding intraclass correlation coefficients (ICC). The outcome measures for the ^1H MRSI data

Table 1
MRI measures in light drinkers (LD) and heavy drinkers (HD) (mean±S.D.)

	LD, n=10	HD, n=12	<i>P</i>	% Difference	Effect size
Total brain tissue volume (ml)	1133±54	1173±107	n.s.	+4	0.50
Brainstem volume (% of brain tissue)	2.44±0.13	2.33±0.12	<0.05	-4	0.90
Normalized midsagittal brainstem area (i.u.)	7.86±0.21	7.24±0.40	<0.0003	-8	2.03
Normalized midsagittal midbrain area (i.u.)	1.85±0.09	1.60±0.20	<0.002	-14	1.68
Normalized midsagittal pons area (i.u.)	1.99±0.17	1.77±0.25	<0.03	-11	1.07
Normalized midsagittal medulla area (i.u.)	3.20±0.21	3.02±0.23	<0.07	-6	0.84

i.u.=institutional units.

were peak areas for NAA, Cho, and Cr, corrected for coil loading and receiver gain, as well as the metabolite peak area ratios NAA/Cr, Cho/Cr, and NAA/Cho. Statistical analyses were performed similar to those described above for MRI data. Age, although not different between the two drinking groups ($P<0.4$), was used as a covariate in all MR analyses due to its possible influence on some of the measures. All values are expressed as mean \pm one standard deviation (S.D.); $P<0.05$ was considered statistically significant.

3. Results

3.1. MRI

As summarized in Table 1, HD compared with LD had smaller normalized brainstem volumes ($P<0.05$) and smaller normalized midsagittal slice areas of the brainstem ($P<0.0003$), midbrain ($P<0.002$), and pons ($P<0.03$). The effect size was greater for the normalized midsagittal area of the brainstem than for the brainstem volume measurement (2.03 vs. 0.90). HD showed no generalized atrophy as reflected in similar total brain tissue volumes for both groups. In addition, total cerebral gray and white matter as well as CSF volumes did not differ between groups.

Secondary analyses using heavy drinking and HIV infection as factors in an ANOVA showed significant main effects of heavy drinking on the same measures as t -tests, except brainstem volume. In addition, a main effect of HIV infection was observed for a larger normalized midsagittal brainstem area ($F_{3,18}=6.19$, $P<0.03$).

The absolute brainstem area on the midsagittal slice was highly correlated with total brainstem volume ($r=0.78$, $P<0.00001$) (Fig. 3). The strengths of the correlations were similar for LD and HD separately (both $r>0.8$, both $P<0.003$).

Area measurements of total midsagittal brainstem and midsagittal midbrain by two independent raters were highly correlated ($r=0.83$ and $r=0.84$, respectively), while midsagittal area measurements of the pons and medulla were not ($r<0.5$). Similarly, ICCs were 0.819 and 0.826 for midsagittal brainstem and midbrain areas, respectively, and below 0.49 for pons and medulla areas. There were no significant corre-

Table 2

Midbrain metabolite ratios and metabolite concentrations (institutional units) in light drinkers (LD) and heavy drinkers (HD) (mean \pm S.D.)

	LD, $n=9$	HD, $n=6$	P
NAA/Cr	2.54 \pm 0.30	2.03 \pm 0.35	<0.014
NAA/Cho	1.65 \pm 0.41	1.76 \pm 0.34	n.s.
Cho/Cr	1.58 \pm 0.26	1.17 \pm 0.23	<0.012
NAA	55.5 \pm 9.6	50.2 \pm 8.0	n.s.
Cho	34.4 \pm 5.6	29.1 \pm 6.2	<0.13
Cr	21.9 \pm 3.1	25.1 \pm 4.3	<0.14

lations between drinking variables and MRI outcome measures.

3.2. MRSI

As summarized in Table 2, HD compared with LD had 20% lower NAA/Cr and 26% lower Cho/Cr (both $P<0.02$) in midbrain/pons spectra, while NAA/Cho was not significantly different. The absolute NAA integral was 10% lower, the Cho integral 17% lower, and the absolute Cr integral 13% higher in HD than LD, but these differences did not reach statistical significances. The greatest effect sizes were observed for NAA/Cr and NAA/Cho (both >1.56), further suggesting that these ratios distinguish the groups better than absolute metabolite measures. No significant effects of heavy drinking were observed for metabolite measures of bilateral hippocampi or mesial temporal lobe white matter, possibly suggesting a preferential vulnerability of the midbrain/pons to chronic alcohol consumption or differences in spectral data quality and variance. No significant correlations were found between drinking variables and metabolite measures.

Secondary 2×2 ANOVAs showed significant main effects of heavy drinking on the same midbrain/pons NAA ratios as t -tests. In addition, a main effect of HIV infection was observed for lower NAA/Cr ($F_{3,10}=31.76$, $P<0.0003$).

4. Discussion

Our MRI findings demonstrate that the brainstem in active chronic heavy drinkers is smaller than in light/non-drinkers despite similar tissue volumes in

the supratentorial cerebrum. This was observed in both area measurements of the brainstem on midsagittal MR images and in traditional volumetric measurements, which were strongly correlated. Furthermore, midsagittal area measurements revealed that the pons and the midbrain, which includes the ventral tegmental area, are the brainstem structures primarily affected by heavy drinking in this sample. Our ^1H MRSI findings of significantly lower NAA/Cr and Cho/Cr in the midbrain/pons region indicate that heavy drinking is associated with neuronal injury and glial changes. Thus, neuronal loss and/or shrinkage of neuronal cell bodies may contribute to brainstem volume loss.

These MR findings support our primary hypothesis of an association in chronic heavy alcohol drinkers between smaller brainstem size and cellular injury.

The strong correlation between midsagittal brainstem area and total brainstem volume supports our hypothesis that midsagittal brainstem area is an accurate estimate of brainstem size. The reproducibility of the midsagittal slice method ($\text{ICC} > 0.819$) was similar to that reported in a cohort of schizophrenic patients for the midbrain (0.957) (Nopoulos et al., 2001) but not for the pons or medulla, the boundaries of which are less well defined on MR images. Midsagittal slice area measurements are a practical alternative to the more labor-intensive volumetric determinations of the entire brainstem and the midbrain. The ease, reproducibility, and reliability of single slice brainstem area measurements should facilitate and encourage future morphometric studies of this brain region.

4.1. MRI

Pathological and neuroimaging studies have demonstrated morphological and functional effects of chronic alcohol consumption in the frontal lobes, parietal and temporal cortices, cerebellum, corpus callosum, thalamus, and hippocampus (Sullivan et al., 2003; Sullivan and Pfefferbaum, 2001; Kril and Halliday, 1999). Recent studies reported alcohol-related pontine abnormalities (Sullivan et al., 2003; Pfefferbaum et al., 2002a); our findings add the midbrain, medulla and overall brainstem to structures disproportionately atrophied and metabolically altered by chronic heavy drinking.

The mechanisms of alcohol-related volume loss are not fully understood, but are likely multifactorial, including induction of apoptosis through destabilization of cell membranes or through dysregulation of the dopaminergic, GABA-ergic, NMDA, serotonergic, and other neurotransmitter systems (Watson, 1992). The effects of ethanol are not consistent: some parts of the brain and some cell types are affected preferentially. In our study of chronic heavy drinkers not in treatment, brainstem volume loss was most pronounced in the midbrain, a structure that contains nuclei with dopaminergic and serotonergic projections critical for the systems modulating reward and affect (Brodie, 2002; Weiss and Porrino, 2002). Thus, the smaller brainstems in heavy drinkers may reflect a decrease in the number of serotonergic neurons (Halliday et al., 1993). Our ^1H MRSI data supports neuronal damage (see below).

Chronic alcohol consumption can also indirectly effect the brain through damage to other systems (e.g. liver) or lead to destructive consequences including poor self-care and stress. Our study participants did not have symptomatic thiamine deficiency (usually secondary to malnutrition). Thiamine deficiency is an established cause of brainstem, subcortical and cortical atrophy and, untreated, may result in Wernicke–Korsakoff syndrome (WKS), a debilitating neurological and cognitive disease. Brainstem abnormalities on MRI related to thiamine deficiency can even be present in asymptomatic chronic alcohol abusers (Sullivan and Pfefferbaum, 2001; Jauhar and Montaldi, 2000; Zubaran et al., 1997; Baker et al., 1996). In addition, pathological studies of chronic alcoholic men with and without WKS revealed up to 78% reduction in the number of brainstem serotonergic neurons and evidence of gliosis compared with controls (Halliday et al., 1993). Preclinical data indicate that serotonin is one of the major neurotransmitters involved in the pathogenesis of alcohol abuse and dependence (Weiss and Porrino, 2002; Heinz et al., 1998; Zhou et al., 1998; Yoshimoto et al., 1996; Li et al., 1993). Furthermore, impairment in serotonin production was posited to be a source of genetic predisposition to alcoholism, and alteration in serotonin levels may predispose to co-morbid affective disorders common in alcohol abuse (Sen et al., 2004; Enoch, 2003; Johann et al., 2003).

Compared with the smaller brainstem associated with chronic heavy drinking, HIV infection was independently associated with a larger brainstem. Thus, inclusion of HIV-infected individuals in our cohort would not increase the probability of type I error. The main alcohol effect on midsagittal brainstem area could have been even greater, were it not for the opposing effect of HIV infection.

4.2. MRSI

Findings from ^1H MRSI of the midbrain/pons region suggest lower NAA, lower Cho, and higher Cr in HD than LD. As absolute metabolite integrals were either increased or decreased in the same pathology, they cannot simply be interpreted to reflect brainstem tissue loss in the spectroscopy volume of interest. All spectra were obtained from a single voxel in the center of each participant's brainstem; all voxels contained solely midbrain and pons (see Fig. 1). Thus, our spectroscopic findings reflect metabolite changes within brainstem tissue, independent of demonstrated volume changes. Specifically, lower NAA measures (20% for NAA/Cr, 10% for NAA) in the midbrain/pons of HD were consistent with our other studies showing low midbrain/pons NAA/Cr in recovering alcoholics in treatment (Gazdzinski et al., 2004). These NAA deficits suggest chronic alcohol-associated injury to brainstem neurons and, thus, possibly reduced afferent dopaminergic and serotonergic output and, indirectly, dysregulation of other alcohol-related neurotransmission, such as GABA, NMDA, and opioids. Abnormalities in either system have been implicated in predisposition to and maintenance of alcohol abuse and dependence (Watson, 1992).

ANOVA showed that HIV infection was also associated with lower NAA/Cr. In contrast to heavy drinking, however, absolute Cho was higher in HIV-positive LD than in HIV-negative LD (39 ± 5 vs. 31 ± 3 , $P=0.02$). This implicates glial alterations possibly associated with inflammatory changes and macrophage infiltration of the brainstem in HIV infection. An enlarged brainstem in HIV infection may reflect the aforementioned pathology, plus axonal swelling and active viral replication as described in neuropathological studies of asymptomatic HIV-positive patients (Tagliati et al., 1998).

Although the number of HIV-positive patients in this sample is small, 2×2 ANOVA suggests additive effects of heavy drinking and HIV infection on NAA/Cr in the midbrain/pons region. This finding is consistent with the literature showing subcortical neuronal injury in both chronic alcoholism and HIV infection (albeit never reported in the brainstem) and with recent studies that suggest that the inflammatory effects of HIV infection on the brain may be compounded by heavy alcohol consumption due to alcohol's own immunosuppressive effects (Meyerhoff, 2001; Pfefferbaum et al., 2002b).

Our study comes with a number of limitations: The emphasis of this study was on effects of heavy drinking evaluated via simple group comparisons between LD and HD; however, we included HIV-positive participants. Results and interpretation of our secondary 2×2 ANOVA should be considered preliminary. When we eliminated HIV-infected individuals from statistical analyses, the magnitude of group differences associated with heavy drinking was not affected, though their statistical significances were somewhat decreased. Second, thiamine deficiency, liver disease, and surreptitious polysubstance use were assessed clinically but, without laboratory data, could not be excluded with certainty. Third, a common limitation of many studies on the chronic effects of alcohol is the retrospective nature of estimated lifetime alcohol consumption, which is less accurate than a prospective diary method and likely underestimates total drinking quantities. Finally, we do not know if the brainstem abnormalities in chronic heavy drinkers preceded heavy drinking or are a consequence of alcohol consumption. Longitudinal studies will be useful in this context.

In conclusion, this study indicates that untreated chronic heavy alcohol use is associated with smaller brainstem size and midbrain/pons neuronal injury. We combined volumetric and spectroscopic data, thereby enhancing the interpretation of the findings in either modality. Our study adds to the emerging evidence of acute brain injury in untreated chronic alcohol drinkers (Meyerhoff et al., 2004; Fein et al., 2003). The results also suggest that asymptomatic HIV infection is associated with brainstem swelling, likely caused by inflammation and gliosis. Finally, we show that brainstem area obtained from a single sagittal

slice through the middle of the brainstem is a reliable approximation of brainstem volume.

Acknowledgement

Major financial support was provided by grant NIH AA10788.

References

- Aylward, E.H., Reiss, A., 1991. Area and volume measurement of posterior fossa structures in MRI. *Journal of Psychiatric Research* 25, 159–168.
- Baker, K.G., Halliday, G.M., Kril, J.J., Harper, C.G., 1996. Chronic alcoholics without Wernicke–Korsakoff syndrome or cirrhosis do not lose serotonergic neurons in the dorsal raphe nucleus. *Alcoholism: Clinical and Experimental Research* 20, 61–66.
- Bhakoo, K.K., Pearce, D., 2000. In vitro expression of *N*-acetyl aspartate by oligodendrocytes: implications for proton magnetic resonance spectroscopy signal in vivo. *Journal of Neurochemistry* 74, 254.
- Brodie, M.S., 2002. Increased ethanol excitation of dopaminergic neurons of the ventral tegmental area after chronic ethanol treatment. *Alcoholism: Clinical and Experimental Research* 26, 1024–1030.
- Cardenas, V.A., Ezekiel, F., Di Sclafani, V., Gomberg, B., Fein, G., 2001. Reliability of tissue volumes and their spatial distribution for segmented magnetic resonance images. *Psychiatry Research: Neuroimaging* 106, 193–205.
- Courchesne, E., Yeung-Courchesne, R., Egaas, B., 1994. Methodology in neuroanatomic measurement. *Neurology* 44, 203–208.
- Duvernoy, H.M., in collaboration with Bonneville, J.F. (Eds.), 1995. *The Human Brain System and Cerebellum: Surface, Structure, Vascularization, and Three-dimensional Sectional Anatomy with MRI*. Springer-Verlag, New York.
- Enoch, M.A., 2003. Pharmacogenomics of alcohol response and addiction. *American Journal of Pharmacogenomics* 3, 217–232.
- Erhardt, S., Schwieler, L., Engberg, G., 2002. Excitatory and inhibitory responses of dopamine neurons in the ventral tegmental area to nicotine. *Synapse* 43, 227–237.
- Fein, G., Di Sclafani, V., Cardenas, V.A., Goldmann, H., Tolou-Shams, M., Meyerhoff, D.J., 2003. Cortical gray matter loss in treatment-naive alcohol dependent individuals. *Alcoholism: Clinical and Experimental Research* 26, 558–564.
- Garnett, M., Corkill, R., Blamire, A., Rajagopalan, B., Manners, D., Young, J.D., Styles, P., Cadoux-Hudson, T.A., 2001. Altered cellular metabolism following traumatic brain injury: a magnetic resonance spectroscopy study. *Journal of Neurotrauma* 18, 231–240.
- Gazdzinski, S., Durazzo, T.C., Meyerhoff, D.J., 2004. Brain recovery during abstinence from alcohol: MRI, MR spectroscopic imaging, and neurocognitive studies. *Neurology* 62; A542 (Suppl. 5).
- Halliday, G., Ellis, J., Heard, R., Caine, D., Harper, C., 1993. Brainstem serotonergic neurons in chronic alcoholics with and without the memory impairment of Korsakoff's psychosis. *Journal of Neuropathology and Experimental Neurology* 52, 567–579.
- Hanstock, C.C., Cwik, V.A., Martin, W.R., 2002. Reduction in metabolite transverse relaxation times in amyotrophic lateral sclerosis. *Journal of the Neurological Sciences* 198, 37–41.
- Heinz, A., Ragan, P., Jones, D.W., Hommer, D., Williams, W., Knable, M.B., Gorey, J.G., Doty, L., Geyer, C., Lee, K.S., Coppola, R., Weinberger, D.R., Linnoila, M., 1998. Reduced central serotonin transporters in alcoholism. *American Journal of Psychiatry* 155, 1544–1549.
- Jauhar, P., Montaldi, D., 2000. Wernicke–Korsakoff syndrome and the use of brain imaging. *Alcohol and Alcoholism* 35, 21–23.
- Johann, M., Bobbe, G., Putzhammer, A., Wodarz, N., 2003. Comorbidity of alcohol dependence with attention-deficit hyperactivity disorder: differences in phenotype with increased severity of the substance disorder, but not in genotype (serotonin transporter and 5-hydroxytryptamine-2c receptor). *Alcoholism: Clinical and Experimental Research* 27, 1527–1534.
- Kilts, C.D., Schweitzer, J.B., Quinn, C.K., Gross, R.E., Faber, T.L., Muhammad, F., Ely, T.D., Hoffman, J.M., Drexler, K.P., 2001. Neural activity related to drug craving in cocaine addiction. *Archives of General Psychiatry* 58, 334–341.
- Kril, J.J., Halliday, G.M., 1999. Brain shrinkage in alcoholics: a decade on and what have we learned? *Progress in Neurobiology* 58, 381–387.
- Kuruoglu, A.C., Arikan, Z., Vural, G., Karatas, M., Arac, M., Isik, E., 1996. Single photon emission computerised tomography in chronic alcoholism. Antisocial personality disorder may be associated with decreased frontal perfusion. *British Journal of Psychiatry* 169, 348–354.
- Li, T.K., Lumeng, L., Doolittle, D.P., 1993. Selective breeding for alcohol preference and associated responses. *Behavior Genetics* 23, 163–170.
- Macmillan, C., Wild, J., Wardlaw, J., Andrews, P., Marshall, I., Easton, V.J., 2002. Traumatic brain injury and subarachnoid hemorrhage: in vivo occult pathology demonstrated by magnetic resonance spectroscopy may not be “ischaemic”. A primary study and review of the literature. *Acta Neurochirurgica* 144, 853–862. (discussion 862).
- Mascalchi, M., Brugnoli, R., Guerrini, L., Belli, G., Nistri, M., Politi, L.S., Gavazzi, C., Lolli, F., Argenti, G., Villari, V., 2002. Single-voxel long TE ¹H-MR spectroscopy of the normal brainstem and cerebellum. *Journal of Magnetic Resonance Imaging* 16, 532–537.
- Meyerhoff, D.J., 2001. Effects of alcohol and HIV infection on the central nervous system. *Alcohol Research and Health: the Journal of the National Institute on Alcohol Abuse and Alcoholism* 25, 288–298.
- Meyerhoff, D.J., Blumenfeld, R., Truran, D., Lindgren, J., Flenniken, D., Cardenas, V., Chao, L.L., Rothlind, J., Studholme, C., Weiner, M.W., 2004. Effects of heavy drinking, binge drinking, and family history of alcoholism on regional brain metabolites. *Alcoholism: Clinical and Experimental Research* 28, 650–661.

- Nopoulos, P.C., Ceilley, J.W., Gailis, E.A., Andreasen, N.C., 2001. An MRI study of midbrain morphology in patients with schizophrenia: relationship to psychosis, neuroleptics, and cerebellar neural circuitry. *Biological Psychiatry* 49, 13–19.
- Pfefferbaum, A., Sullivan, E.V., Mathalon, D.H., Shear, P.K., Rosenbloom, M.J., Lim, K.O., 1995. Longitudinal changes in magnetic resonance imaging brain volumes in abstinent and relapsed alcoholics. *Alcoholism: Clinical and Experimental Research* 19, 1177–1191.
- Pfefferbaum, A., Rosenbloom, M.J., Serventi, K.L., Sullivan, E.V., 2002a. Corpus callosum, pons, and cortical white matter in alcoholic women. *Alcoholism: Clinical and Experimental Research* 26, 400–406.
- Pfefferbaum, A., Rosenbloom, M.J., Sullivan, E.V., 2002b. Alcoholism and AIDS: magnetic resonance imaging approaches for detecting interactive neuropathology. *Alcoholism: Clinical and Experimental Research* 26, 1031–1046.
- Piccio, M.R., Corrigan, W.A., 2002. Neuronal systems underlying behaviors related to nicotine addiction: neural circuits and molecular genetics. *Journal of Neuroscience* 22, 3338–3341.
- Raz, N., Torres, I.J., Spencer, W.D., White, K., Acker, J.D., 1992. Age-related regional differences in cerebellar vermis observed in vivo. *Archives of Neurology* 49, 412–416.
- Scroop, R., Sage, M.R., Voyvodic, F., Kat, E., 2002. Radiographic imaging procedures in the diagnosis of the major central neuropathological consequences of alcohol abuse. *Australasian Radiology* 46, 146–153.
- Sen, S., Villafuerte, S., Nesse, R., Stoltenberg, S.F., Hopcian, J., Gleiberman, L., Weder, A., Burmeister, M., 2004. Serotonin transporter and GABAA alpha 6 receptor variants are associated with neuroticism. *Biological Psychiatry* 55, 244–249.
- Skinner, H.A., 1979. A multivariate evaluation of the MAST. *Journal of Studies on Alcohol* 40, 831–844.
- Skinner, H.A., Sheu, W.J., 1982. Reliability of alcohol use indices: the lifetime drinking history and the MAST. *Journal of Studies on Alcohol* 43, 1157–1170.
- Sobell, L.C., Sobell, M.B., Riley, D.M., Schuller, R., Pavan, D.S., Cancilla, A., Klajner, F., Leo, G.I., 1988. The reliability of alcohol abusers' self-reports of drinking and life events that occurred in the distant past. *Journal of Studies on Alcohol* 49, 225–232.
- Soher, B.J., Young, K., Govindaraju, V., Maudsley, A.A., 1998. Automated spectral analysis: III. Application to in vivo proton MR spectroscopy and spectroscopic imaging. *Magnetic Resonance in Medicine* 40, 822–831.
- Soher, B.J., Vermathen, P., Schuff, N., Wiedermann, D., Meyerhoff, D.J., Weiner, M.W., Maudsley, A.A., 2000. Short TE in vivo ¹H MR spectroscopic imaging at 1.5 T: acquisition and automated spectral analysis. *Magnetic Resonance Imaging* 18, 1150–1165.
- Sullivan, E.V., Pfefferbaum, A., 2001. Magnetic resonance relaxometry reveals central pontine abnormalities in clinically asymptomatic alcoholic men. *Alcoholism: Clinical and Experimental Research* 25, 1206–1212.
- Sullivan, E.V., 2000. NIAAA Research Monograph No. 34, Chapter 14: Human brain vulnerability to alcoholism: Evidence from neuroimaging studies, in Noronha A, Eckardt M, Warren K (eds): Review of NIAAA's neuroscience and behavioral research portfolio. pp. 473–508.
- Sullivan, E.V., Rosenbloom, M.J., Serventi, K.L., Deshmukh, A., Pfefferbaum, A., 2003. Effects of alcohol dependence comorbidity and antipsychotic medication on volumes of the thalamus and pons in schizophrenia. *American Journal of Psychiatry* 160, 1110–1116.
- Sziraki, I., Sershen, H., Hashim, A., Lajtha, A., 2002. Receptors in the ventral tegmental area mediating nicotine-induced dopamine release in the nucleus accumbens. *Neurochemical Research* 27, 253–261.
- Tagliati, M., Simpson, D., Morgello, S., Clifford, D., Schwartz, R.L., Berger, J.R., 1998. Cerebellar degeneration associated with human immunodeficiency virus infection. *Neurology* 50, 244–251.
- Watson, R.R. (Ed.), *Alcohol and Neurobiology: Receptors, Membranes and Channels*. CRC Press, Boca Raton, FL, pp. 1–303.
- Weiss, F., Porrino, L.J., 2002. Behavioral neurobiology of alcohol addiction: recent advances and challenges. *Journal of Neuroscience* 22, 3332–3337.
- Yoshimoto, K., Yayama, K., Sorimachi, Y., Tani, J., Ogata, M., Nishimura, A., Yoshida, T., Ueda, S., Komura, S., 1996. Possibility of 5-HT₃ receptor involvement in alcohol dependence: a microdialysis study of nucleus accumbens dopamine and serotonin release in rats with chronic alcohol consumption. *Alcoholism: Clinical and Experimental Research* 20, 311A–319A.
- Zhou, F.C., McKinzie, D.L., Patel, T.D., Lumeng, L., Li, T.K., 1998. Additive reduction of alcohol drinking by 5-HT_{1A} antagonist WAY 100635 and serotonin uptake blocker fluoxetine in alcohol-preferring P rats. *Alcoholism: Clinical and Experimental Research* 22, 266–269.
- Zubaran, C., Fernandes, J.G., Rodnight, R., 1997. Wernicke–Korsakoff syndrome. *Postgraduate Medical Journal* 73, 27–31.